

Supporting information for

**IGF-Loaded Silicon and Zinc Doped Brushite Cement: Physico-Mechanical
Characterization and *In Vivo* Osteogenesis Evaluation**

SaharVahabzadeh¹, AmitBandyopadhyay¹and Susmita Bose^{1*}

¹W. M. Keck Biomedical Materials Research Laboratory, School of Mechanical and Materials Engineering, Washington State University, Pullman, WA 99164-2920, USA

Rakesh Mandal² and Samit Kumar Nandi²

²Department of Veterinary Surgery and Radiology, West Bengal University of Animal and Fishery Sciences, Kolkata-700037, India, Email- samitnandi1967@gmail.com

* Corresponding Author:

Susmita Bose,

Professor, School of Mechanical and Materials Engineering, Affiliate Professor, Department of Chemistry, Washington State University, Pullman, WA 99164-2920

Phone: (509) 335-7461, Fax: (509) 335-4662 Email- sbose@wsu.edu

1. Materials and Methods

1.1. Cement Preparation

The brushite cements were synthesized as described elsewhere [1]. Briefly, monocalcium phosphate monohydrate (MCPM, $\text{Ca}(\text{H}_2\text{PO}_4)_2 \cdot \text{H}_2\text{O}$, Sigma Aldrich, USA) and β - tricalcium phosphate (β -TCP, β - $\text{Ca}_3(\text{PO}_4)_2$, as-synthesized) were mixed at a molar ratio of 1:1. The final mixture of cement was composed of 42 wt. % fine β -TCP, 31 wt. % granular β -TCP, 21 wt. % MCPM, and 5 wt. % magnesium hydrogen phosphate trihydrate ($\text{MgHPO}_4 \cdot 3\text{H}_2\text{O}$, Sigma Aldrich, USA). Small amounts of magnesium sulphate (MgSO_4 , Sigma Aldrich, USA) and sodium hydrogen phosphate ($\text{Na}_2\text{H}_2\text{P}_2\text{O}_7$, Sigma Aldrich, USA) were also added to modify the setting time [2,3]. 0.5 wt. % Si, 0.25 wt. % Zn, and 0.5 wt. % Si/0.25 wt. % Zn doped brushite cements were made by mixing relative amount of SiO_2 and ZnO with precursors of β -TCP. The cement paste was prepared by mixing 2 wt. % polyethylene glycol (PEG) solution with the powder. The polymer concentration and powder to liquid ratio (P/L) of 3.33:1 was selected based on our previous work [1]. Cement paste was then molded into 6mm diameter and 12 mm height cylindrical molds and were kept under 100% humidity condition for one hour. Finally, they were immersed in PBS for 24 hour at 37 °C. From now on pure, 0.5 wt. % Si, 0.25 wt. % Zn, and 0.5 wt. % Si/0.25 wt. % Zn doped brushite cements will be denoted as BrC, Si-BrC, Zn-BrC, and Si/Zn-BrC, respectively.

1.2. Phase Analysis, Microstructure, and Mechanical Properties

Phase analysis of pure and doped BrCs was carried out by Siemens D500 Krystalloflex X-ray diffractometer (XRD) using Cu K α radiation at 30 mA and 35 kV at room temperature, over the 2θ range between 10° and 40° at a step size of 0.1° and a count time of 1 sec per step. β -TCP wt. % in cements was determined using the relative intensity ratio of the corresponding major phases using the following relation:

*Percent of the phase to be determined = relative intensity ratio of the phase * 100*

$$\text{Relative intensity ratio} = \frac{\text{Intensity of the major peak of the phase to be determined}}{\Sigma \text{ Intensity of major peaks of all the phases}}$$

The surface morphology of the BrCs was characterized using a field emission scanning electron microscope (FESEM) (FEI Inc., OR, USA). A screw-driven universal testing machine (AG-IS, Shimadzu, Japan) with a constant crosshead speed of 0.33 mm/min was used to measure compressive strength of pure and doped BrCs. Compressive strength was calculated using the maximum recorded load and the sample dimensions. Compressive strength was tested on at least seven samples for each composition.

2. Results

2.1. *Radiological Examination*

Figure 1S shows the radiographs of cement implanted rabbit distal femur after 1 and 3 months post implantation. After 1 month, there was no appreciable change in radiodensity and size of all groups except Si/Zn-BrC. However, at 3 months, the radiograph of all doped BrCs showed reduction in size and radiodensity of the implant.

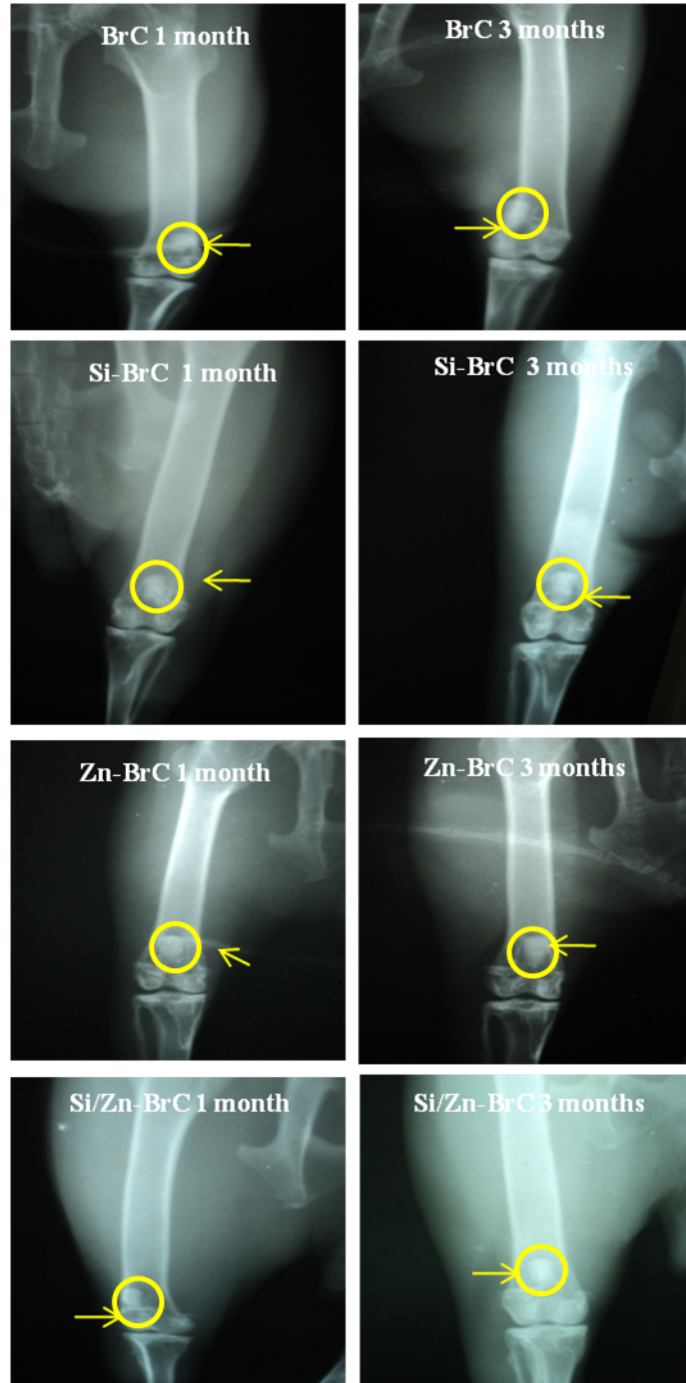


Figure 1S-X-ray images depicting implanted BrCs in the distal femur after 1 and 3 months (arrow shows the implantation site and subsequent bone formation).

Figure 2S shows the radiographs of IGF-1 loaded BrCs in rabbit femoral defect after 1 and 3 months post implantation. After 1 month, BrC-IGF-1 radiograph showed establishing continuity in the medullary cavity. At 3 months, radiographs showed perceptible change of radiodensity of

implant material in bony defect and continuity of the marrow cavity in the adjacent area of defect was more ascertainable. Si-BrC-IGF-1 radiograph showed the gradual decrease in radiodensity after 1 month post implantation. No significant change in radiodensity of Zn-BrC-IGF-1 was found at 1 month post implantation. However, the process of remodeling of medullary cavity started at 3 months.

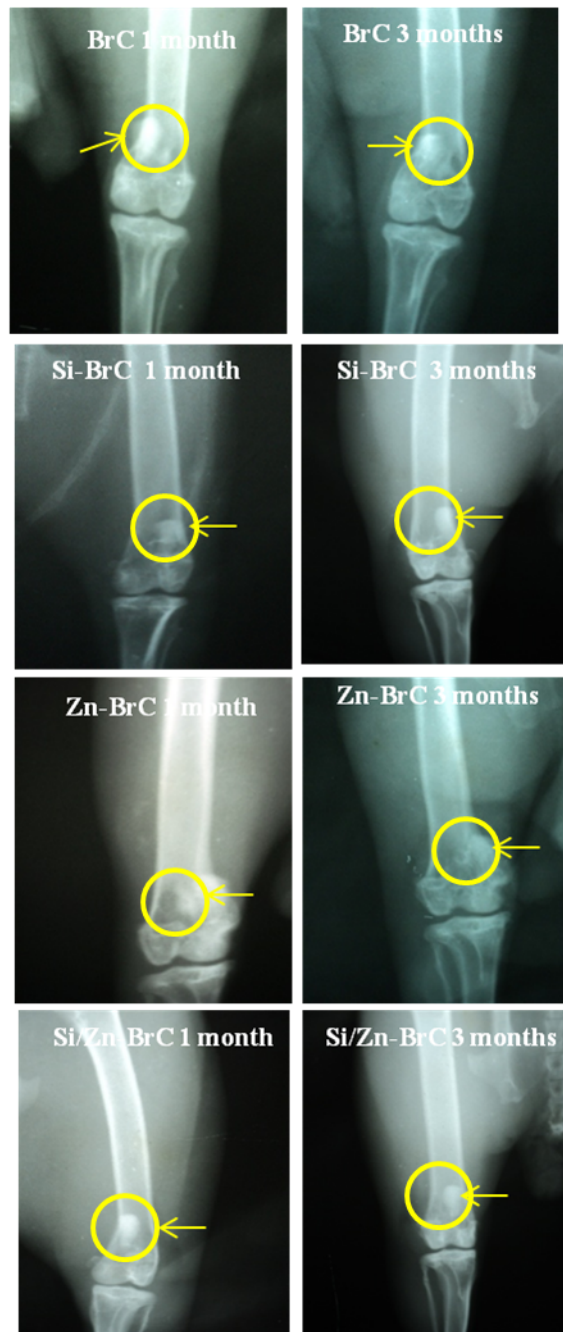


Figure 2S-X-ray images depicting IGF-1 loaded BrCs implanted in the distal femur after 1 and 3 months (arrow shows the implantation site and subsequent bone formation).

2.2. Microstructural Examination

Figure 3S shows the SEM images at the bone-implant interface of doped BrCs after 2 and 4 months of post implantation. As shown in **Figures 3S-A₁ and A₂**, BrC showed amorphous phase of cement where new bone formation was initiated from all sides. Dissolution and recrystallization process were occurring along with presence of amorphous like structure. In comparison to BrC, there was no interfacial gap between bone and Si-BrC. Degradation of cement and new bone formation was initiated (**Figures 3S-B₁ and B₂**). Zn-BrC revealed no association of the grafted material with the bony structure in the interface as observed by presence of interfacial gap. Collagen fibrils were present on the cement surface (**Figures 3S-C₁ and C₂**). **Figures 3S-D₁ and D₂** show the SEM images of Si/Zn-BrC with close association of the grafted material with the host bone in the interface. Compared to 2 months, lesser interfacial gap with approximate size of 5-10 μm between bone and pure BrC was noticed. Collagen fibril was present within the bone (**Figures 3S-E₁ and E₂**). However, complete absence of interfacial gap between the grafted material and host bone was noticed in all three doped BrCs (**Figures 3S-F₁ to H₂**). Discrete collagen fibril formation and amorphous structure in Si-BrC and Zn-BrC along with presence of new osseous tissue near the vicinity of cortical bone was noticed. In addition, new bone was formed in the grafted side of Si/Zn-BrC.

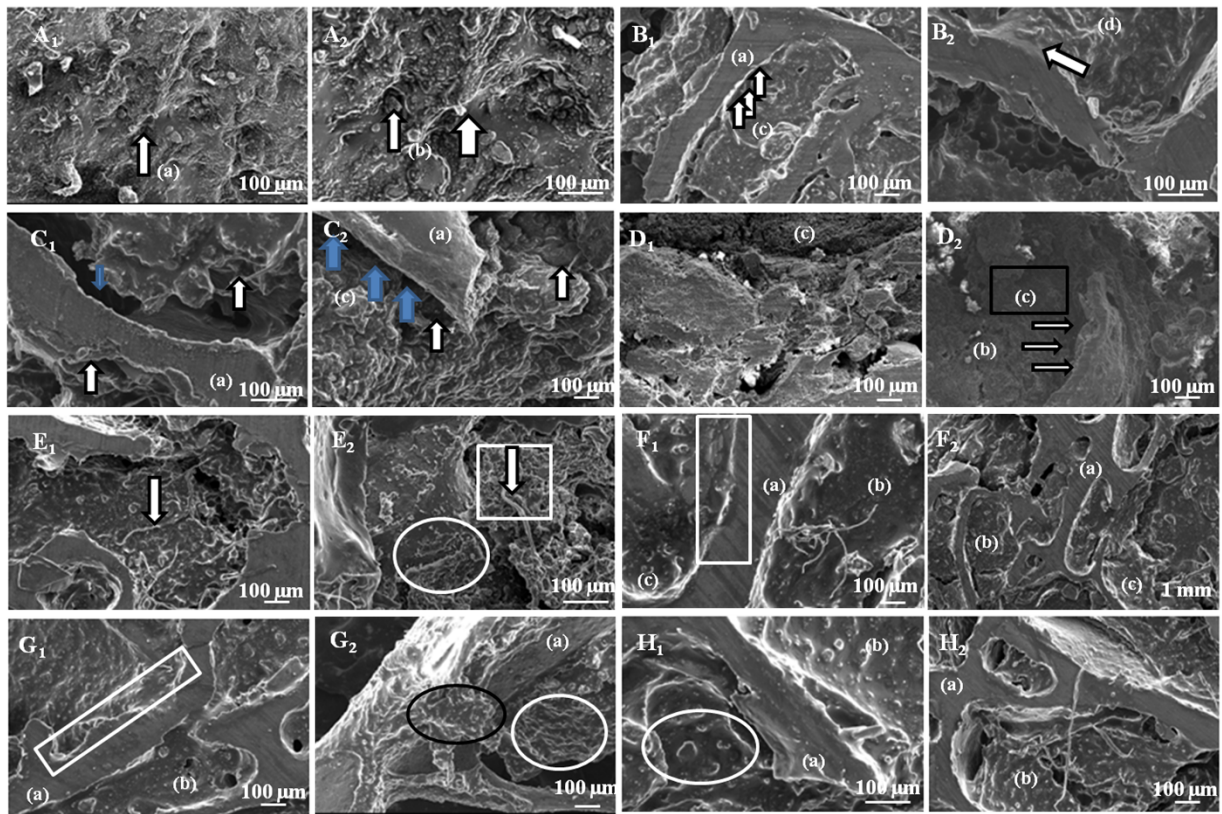


Figure 3S- SEM images of implanted cements after 2 and 4 months post implantation.

A₁ and A₂) Pure BrC- (a) Amorphous cement phase (b) cement pores,

B₁ and B₂) Si-BrC - (a) Cortical bone (b) Material (c) New bone formation (d) No interfacial gap,

C₁ and C₂) Zn-BrC- White arrow: Collagen fibrils Blue arrow: Interfacial gap (a) Cortical bone,

D₁ and D₂) Si/Zn-BrC - (a) Normal bony structure (b) Close association of the grafted material (c) Dissolution and re-crystallization process initiated.

E₁ and E₂) Pure BrC - White arrow: Collagen, White circle: Cement material, White box: New osseous tissue formation, (a) Normal bony structure,

F₁ and F₂) Si-BrC- (a) Normal bone, (b) Material, (c) Diffused new bony tissue, White box: No interfacial gap, White arrow: Discrete collagen fiber,

G₁ and G₂) Zn-BrC- (a) Normal bone, (b) Material, White box: No interfacial gap, Black box: New osseous tissue, White circle: Collagen fibril formation towards host bone,

H₁ and H₂) Si/Zn-BrC- (a) Normal bone, (b) Material, White circle: New bone formation, White box: No interfacial gap.

Figure 4S shows the SEM images at the bone-implant interface of IGF-1 loaded pure and doped BrCs at 2 and 4 months of post implantation. Pure BrC-IGF-1 showed formation of soft bone tissues along with presence of network like matured osteoblastic cells and tissues without any interfacial gap after 2 months of post implantation, as shown in **Figures 4S-A₁ and A₂**. Sporadic amorphicity in the implanted cement site was also found. After 4 months post implantation, no specific change was observed in BrC-IGF-1 sample, as shown in **Figures 4S-E₁ and E₂**. Si-BrC-IGF-1 samples showed presence of granulation of cement along with filopodia of the bone cells after 2 months post implantation and matured bone cells were seen mostly in contact site from the bone as shown in **Figures 4S-B₁ and B₂**. At 4 months, matured bone tissues were observed not only from the contour of intact bone, but also throughout the implanted site by the cement. Mesopores observed at 2 months in the cement site were almost closed. Collagen fibrils were found sporadically on the cement site and interfacial gap between the cement site and bone contour was absent (**Figures 4S-F₁ and F₂**). In Zn-BrC-IGF-1 as shown in **Figures 4S-C₁ and C₂**, the cementous portion was amorphous and more interfacial gap was found compared to the other compositions after 2 months. At 4 months, Interfacial gap was almost covered and scanty granular tissue was observed. In addition, osteoblastic tissues with collagen network were found throughout the cement site (**Figures 4S-G₁ and G₂**). Huge CaP crystals throughout the cement site were found in Si/Zn-BrC-IGF-1 at 2 months. Dissolution and reprecipitation of cement site was almost complete, along with formation of homogenous bone soft tissues. In addition, interfacial gap was almost covered and underlying collagen network was found, but not abundantly (**Figures 4S-D₁ and D₂**). However, as shown in **Figures 4S-H₁ and H₂**, there was complete bone maturation at the cement with no interfacial gap at 4 months. In addition, abundant collagen network was seen.

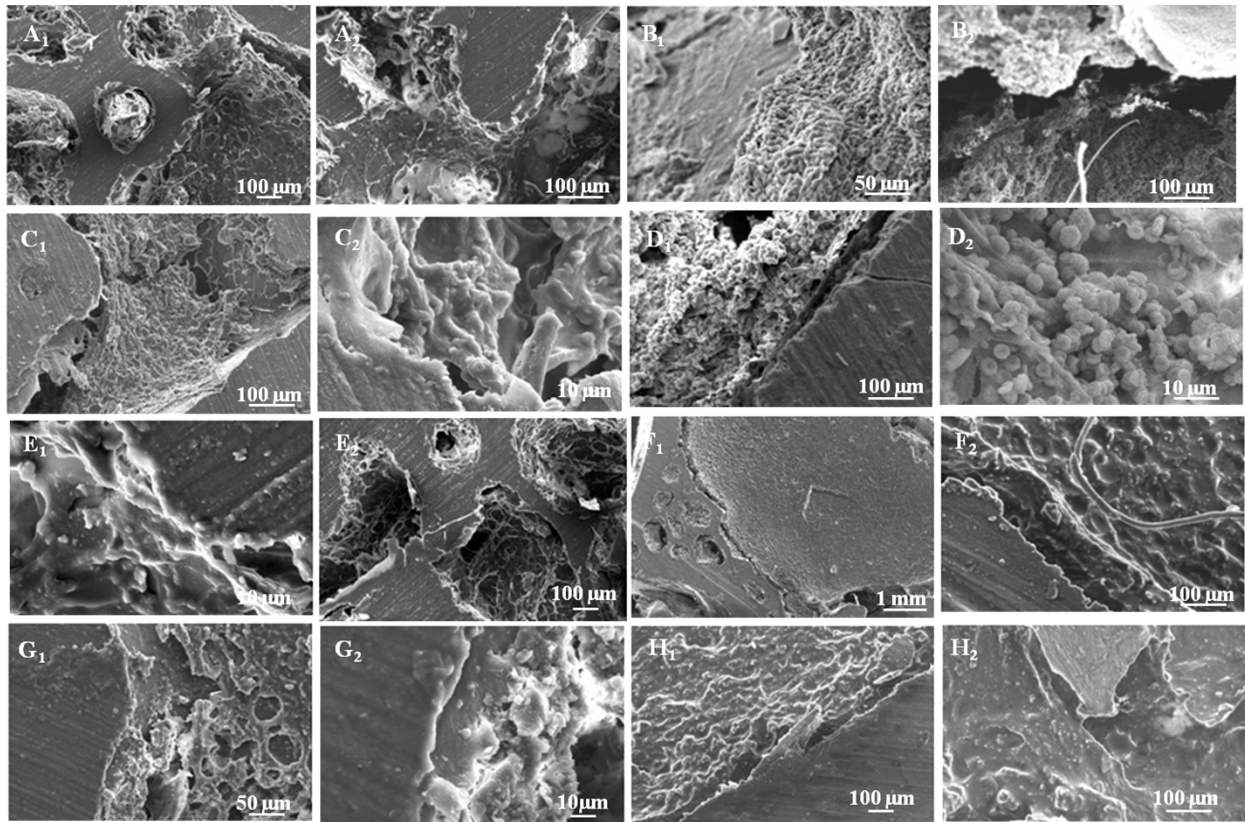


Figure 4S- SEM images of IGF-1 loaded cements after 2 and 4 months post implantation.

¹M. Roy, K. DeVoe, A. Bandyopadhyay, S. Bose, Mechanical property and in vitro biocompatibility of brushite cement modified by polyethylene glycol, *Mater. Sci. Eng. C*, 2012, 32, 2145–2152..

² M. Bohner, F. Theiss, D. Apelt, W. Hirsiger, R. Houriet, G. Rizzoli, E. Gnos, C. Frei, J. A. Auer, B. von Rechenberg, Compositional changes of a dicalcium phosphate dihydrate cement after implantation in sheep, *Biomaterials*, 2003, 24, 3463–74.

³ M. Bohner, J. Lemaitre, T. A. Ring, Effects of sulfate, pyrophosphate, and citrate ions on the physicochemical properties of cements made of β -tricalcium phosphate-phosphoric acid-water mixtures, *J. Am. Ceram. Soc.*, 1996, 79, 1427–1434.